ORIGINAL ARTICLE

European Journal of **Soil Science** WILEY

Influence of soil structure on the spread of *Pseudomonas fluorescens* in soil at microscale

Archana Juyal[1,2,3] | Wilfred Otten[1,4] | Philippe C. Baveye[5] |
Thilo Eickhorst[2]

[1]School of Science Engineering and Technology, Abertay University, Dundee, UK

[2]FB 2 (Biology/Chemistry), University of Bremen, Bremen, Germany

[3]Department of Plant, Soil and Microbial Sciences, Michigan State University, East Lansing, Michigan

[4]School of Water, Energy and Environment, Canfield University, Cranfield, UK

[5]ECOSYS Unit, AgroParisTech, Université Paris-Saclay, Thiverval-Grignon, France

Correspondence
Thilo Eickhorst, FB 2 (Biology/Chemistry), University of Bremen, Bremen, Germany.
Email: eickhorst@uni-bremen.de

Abstract

For over a half a century, researchers have been aware of the fact that the physical and chemical characteristics of microenvironments in soils strongly influence the activity, growth and metabolism of microorganisms. However, many aspects of the effect of soil physical characteristics, such as the pore geometry, remain poorly understood. Therefore, the objective of the present research was to determine the influence of soil pore characteristics on the spread of bacteria, observed at the scale relevant to microbes. *Pseudomonas fluorescens* was introduced in columns filled with 1–2 mm soil aggregates, packed at different bulk densities. Soil microcosms were scanned at 10.87 μm voxel resolution using X-ray computed tomography (CT) to characterize the geometry of pores. Thin sections were prepared to determine the spread and colonization of bacteria. The results showed that average bacterial cell density was 174 cells mm^{-2} in soil with bulk density of 1.3 g cm^{-3} and 99 cells mm^{-2} in soil with bulk density of 1.5 g cm^{-3}. Soil porosity and solid-pore interfaces influence the spread of bacteria and their colonization of the pore space at lower bulk density, resulting in relatively higher bacterial densities in larger pore spaces. The study also demonstrates that thin sectioning of resin-impregnated soil samples can be combined with X-ray CT to visualize bacterial colonization of a 3D pore volume. This research therefore represents a significant step towards understanding how environmental change and soil management impact bacterial diversity in soils.

Highlights

- We used a quantitative approach to study bacterial spread in soil at scales relevant to microbes.
- The rate of pseudomonas spread decreased with increased bulk density of soil.
- Soil porosity and soil-pore interface influence *Pseudomonas* in lower bulk density soil.
- Soil structure with different pore characteristics effects spread and activity of bacteria in soil.

1 | INTRODUCTION

Soil microorganisms are intimately involved in numerous processes occurring in soils, including the supply of nutrients to plants, the stimulation of plant growth through production of growth hormones, controlling the activity of plant pathogens, maintaining soil architecture, and contributing to the leaching of inorganics and the mineralization of organic pollutants (Baveye et al., 2018; Burd, Dixon, & Glick, 2000; Hayat, Ali, Amara, Khalid, & Ahmed, 2010; Zaidi, Khan, Ahemad, & Oves, 2009; Zhuang, Chen, Shim, & Bai, 2007). These microbial communities have immense metabolic and physiological heterogeneity, which enables them to live, adapt and proliferate in soil environments that also exhibit an extremely high level of structural and chemical heterogeneity (Madigan, Clark, Stahl, & Martinko, 2010). Despite the relatively high bacterial abundance in fertile soil, bacteria occupy only a small fraction of the soil surfaces (Young, Crawford, Nunan, Otten, & Spiers, 2008). In soil, microorganisms tend to aggregate (Ekschmitt, Liu, Vetter, Fox, & Wolters, 2005), forming microbial hotspots in very small volumes of soil (<1 cm^3). In a review, Kuzyakov and Blagodatskaya (2015) argue that most of the biogeochemical processes are taking place in these hotspots. Such hotspots are transient in nature and originate from complex interactions between physical, chemical and microbial processes. Examples of such hotspots of activity include the rhizosphere, the detritusphere and the surface of soil aggregates. Of these examples of hotspots, the rhizosphere is the most dynamic, with hotspots lasting days, whereas hotspots associated with soil structure can be more persistent and last for months.

Hotspots of microbial activity do not exist in isolation. A colocation of various conditions is required for the aforementioned processes to occur. Soil pores play a significant role in formation of such hotspots as soil architecture forms an interconnected network through which various processes, including diffusion of oxygen, transport of enzymes and dissolved organic matter, mobility of bacteria and interaction between bacterial species, occur. A number of researchers have observed spatial patterns in the distribution of bacteria at a microhabitat scale (Kizungu et al., 2001; Nunan, Wu, Young, Crawford, & Ritz, 2003; Vieublé Gonod, Chadoeuf, & Chenu, 2006). For example, Vieublé Gonod et al. (2006) observed a heterogeneous pattern of mineralization of 2,4-D (2,4 Dichlorophenoxyacetic acid) in a soil, with an increase in variability when going from field to microhabitat scale.

An explanation is that bacteria are not randomly distributed and are located in different microenvironments (i.e., mainly located in pores of different sizes and shapes) in soil.

Despite the fact that soil structure plays a regulating role in most of these processes, studying these processes at the microscale is hampered by the opacity of soils and inability of single technology to visualize all processes that are involved. As such, we have little knowledge about movement by bacteria from a local microsite in soil and how this is affected by physical characteristics such as pore structure. It is essential to understand the exact mechanisms that are involved in microbial processes (e.g., hotspots occurrence) in order to predict their cumulative effect at a large scale. No single technology is available to address this issue, but it could be addressed through the application of multiple techniques to bring together physical, chemical and biological characterization. The merging of various technologies has received great attention in recent years (Baveye et al., 2018; Hapca, Baveye, Wilson, Lark, & Otten, 2015; Juyal et al., 2019; Schlüter et al., 2018).

In this study we apply such integrative imaging approaches to study how bacteria move in soil and how soil structure regulates the spatial distribution of bacteria. Our key objective is to analyse the influence of soil architecture on the extent of spread of bacteria in soil from a localized spot at the microscale. We investigated this by quantifying the spatial distribution of *Pseudomonas fluorescens* following introduction into microcosms with controlled structural properties by examining soil thin sections and quantifying the characteristics of soil pore space using X-ray computed tomography (CT). Through X-ray CT we determine pore space characteristics such as porosity, which quantifies the total volume available to microbial interactions and growth, the connectivity of pores, which indicates how accessible the pore volume is for organisms with regard to interaction and food sources, and the pore-solid interface area, which effectively defines the surface area accessible to microorganisms in soils.

This allowed us to test the following hypotheses related to the impact of soil structure on spatial distribution of bacteria in soil.

1. Bacterial densities increase in a small volume surrounding nutrient sources.
2. The extent of high bacterial density around nutrient sources reduces with increasing bulk density due to reduced mobility and diffusion.

3. Soil porosity, pore connectivity and the soil-pore interface influence the spread and colonization of bacteria.

2 | MATERIALS AND METHODS

2.1 | Soil sampling and preparation

Soil samples used in this study originated from a sandy loam soil collected in 2011 at an experimental site, Bullion field, situated within the James Hutton Institute in Invergowrie, Scotland. The soil was air-dried and soil aggregates were sieved down to an aggregate size of 1–2 mm and stored in a cold room (4°C). The physicochemical characteristics of the selected soil aggregate fraction (1–2 mm) are as follows: sand, 55.7%; silt, 31.0%; clay, 13.3%; organic matter, 5.5%; C/N ratio, 17.1. For the experiment, the soil was sterilized by autoclaving twice (moist heat) in glass bottles at 121°C at 100 kPa for 30 min with a 24-hr interval time. The aggregate size of 1–2 mm was selected based on a previous study (Juyal et al., 2018).

2.2 | *Pseudomonas fluorescens* inoculum preparation

Pseudomonas fluorescens cells (SBW25) were used as bacterial inoculum. *Pseudomonas* was grown on King's B medium (KB, 10 g glycerol, 1.5 g K_2HPO_4, 1.5 g $MgSO_4.7H_2O$, 20 g Proteose peptone No.3 (Becton, Dickinson & Company, Wokingham, UK), 15 g technical agar (1.5% w/v) per litre) (King et al., 1954).

For each experiment, an overnight culture was prepared by transferring a loop-full of colony in 10 mL of sterile broth and incubated at 28°C on a shaker at 200 rpm for 24 hr. The cells were harvested by centrifugation (4,000 g) for 5 min and resuspended in 10 mL phophate buffered saline (PBS) solution to a final concentration of $OD_{600} = 0.95$.

To provide a reproducible source of inoculum to introduce bacteria into the soil, an agarose pellet was used as described in Juyal et al. (2018). Briefly, a 1,000-μL inoculum of washed cells (see above) was mixed with 30 mL of 1.5% LMP agarose solution (Fisher Bioreagents, Loughborough, UK; gelling point ≤35°C). After pouring a layer of approximately 2 mm height into a sterile petri dish, sterile glass beads (2 mm in diameter) were sparsely placed on the solidified agarose. Subsequently, they were covered by additional agarose to a final height of 5 mm. The solidified agarose was then cut into small cylindrical-shaped pellets (referred to as an inoculum pellet) using the circular end of a 1-mL pipette tip. Each pellet was 3.5 mm in diameter and ca. 4 mm in height and contained a glass bead in its centre (Figure S1). The glass

beads were used to ensure that the location of inoculation could be identified via X-ray CT scanning and in soil thin sections. Control pellets without bacteria were prepared in a similar way.

2.3 | Preparation of soil microcosms

The effect of structure on the spread of bacteria was studied by preparing microcosms in polyethene rings of size 3.4 cm^3 (inner diameter 17.0 mm and height 15.0 mm) packed at two soil bulk densities, 1.3 and 1.5 g cm^{-3}. Previous work showed that these densities give significant differences in pore geometry (Juyal et al., 2019). The moisture content of the soil was adjusted to 60% pores filled with water for all samples. The amount of water added to soil to acquire 60% water filled pores was 0.224 cm^3 g^{-1} for bulk density of 1.3 g cm^{-3} and 0.1569 cm^3 g^{-1} for bulk density of 1.5 g cm^{-3}. The total porosity of soil at bulk density of 1.3 g cm^{-3} was 48% and 40% for soil packed at bulk density of 1.5 g cm^{-3}.

Soil was transferred in these rings in two layers, covering half the height each. After packing the bottom half of the soil, an inoculum pellet was placed on top of the soil layer in its centre and then covered with the second half of the soil. Control samples with the sterile inoculum pellet were packed in a similar way. Three replicates per treatment were prepared, producing 12 soil microcosms in total. The microcosms were incubated at 23°C in the dark to allow bacteria to grow and spread in soil. The soil microcosms were sampled after an incubation period of 14 days.

2.4 | Impregnation of soil microcosms

The impregnation of soil microcosms was carried out according to the protocol of Juyal et al. (2019). Briefly, the samples were fixed overnight with 2% formaldehyde solution (v/v in H_2O; 37% stock solution, Sigma Aldrich, Taufkirchen, Germany) at 4°C. The samples were washed in millipore quality distilled water and dehydrated with a graded series (50, 70, 90 and three changes of 100%) acetone (technical grade, VWR) to avoid interference with the polymerization of resin. The acetone-saturated samples were kept under vacuum (280 mbar) to facilitate the entire exchange of all pores.

An impregnation mixture (2 L) was prepared by amending 1.4 L of polyester resin (Palatal P50-01, Büfa, Germany) with 2,240 μL of co-accelerator (1.6‰ (v/v) 1%-Cobalt Octoate accelerator, Oldopal, Büfa, Germany) and 4,480 μL of hardener (3.2‰ (v/v) cyclohexanone peroxide, Cologne, Akzo Nobel, Germany). After amending, 500 mL of acetone were added as a thinner, mixed well

and the resin mixture was kept under vacuum (240 mbar) to remove gas bubbles before adding it to the samples. Acetone was removed from the container with samples that were subsequently transferred into a desiccator equipped with a tube and a valve connected to the resin mixture. The resin mixture was added slowly under vacuum (240 mbar) to allow an infiltration of microcosms with resin from the bottom to the top to ensure that the pores of the soil were filled with resin mixture as completely as possible. Shortly before reaching the surface of the microcosms (after approx. 45 min) the addition of resin was stopped for a while and the vacuum was increased (200 mbar) for 1 hr to remove the gaseous phase from the soil pores carefully. Finally, the remaining mixture was added to cover the samples completely with resin. Samples were left at room temperature under a hood for polymerization of the resin, which lasted 9 days.

After polymerization, excess resin and the polyethylen (PE) rings of samples were removed to produce a cylindrically shaped resin-impregnated soil sample. A straight vertical cut was made on the edge of each sample using a diamond saw (Woco 50, Conrad, Clausthal-Zellerfeld, Germany) to ensure the starting point of the scan is the same for all samples while scanning under X-ray CT.

2.5 | X-ray CT scanning of impregnated microcosms

The impregnated samples were scanned using a Metris X–Tek HMX CT scanner (NIKON Metrology, Tring, UK). Samples were scanned at 10.87 μm voxel resolution with energy settings of 200 keV and 56 μA and 2000 angular projections. The straight vertical cut was used as a reference side facing the gun of the CT scanner for each scan to facilitate alignment for image processing. A tungsten target with a 0.25-mm aluminium filter was used. Reconstruction of radiographs into 3D volumes was performed using Metris X-Tek software CT Pro v2.1 (NIKON Metrology). A volume processing software, VGStudio MAX V2.2 (Volume Graphics, Heidelberg, Germany), was used to change contrast in reconstructed volumes and to export image stacks (*bmp format) for further processing.

2.6 | Preparation of soil thin sections

After X-ray CT scanning, three soil thin sections were prepared for cell counting from each individual resin-impregnated soil microcosm. One thin section passed through the centre of the glass bead and the others approximately 2.5 mm away from the bead (Figure S2). To prepare soil thin sections, the reference side of the soil block (opposite side of the vertical cut described above) was glued onto a petrographic slide of size 27 × 46 mm and thickness 0.15 mm (Beta Diamonds Inc., Yorba Linda, CA, USA) with epoxy resin (Epofix resin, Ballerup, Struers, Denmark). An estimated distance of each thin section from the reference slide was calculated by measuring the distance between the reference side and the glass bead in X-ray CT grey scale images. Samples were cut and polished using a diamond-coated saw and cupwheel grinder (Discoplan TS, Struers). A frosted petrographic slide was glued on to the polished surface of the sample. Subsequently, the opposite side of the sample was cut and the sample was polished to a final thickness of approx. 30 μm.

The final thickness of each thin section was measured with a micrometer (1 μm accuracy), considering the thickness of the slide and the amount of glue added. The measured values were used to determine the exact position of the prepared soil thin sections within the scanned sample. The thin sections were referred to as II (through centre of bead), I and III (approximately 2.5 mm above and below the bead towards the reference side, respectively).

2.7 | Enumeration of bacteria in soil thin sections

For enumeration of bacterial cells, a drop of mounting medium containing 1.5 μg mL^{-1} of DAPI stain (Vectashield H-1200, Vector Laboratories, Burlingame, CA, USA) was applied on top of the soil thin sections and covered with a cover slip of size 27 × 46 mm (Beta Diamonds Inc.). Bacterial cells were observed with an Olympus BX61 fluorescence microscope (Olympus, Tokyo, Japan) equipped with a 100 W Hg vapour lamp (HBO 102 W/2, Munich, Osram, Germany), using a 100× objective lens (UPlanSApo, Olympus). DAPI-stained bacterial cells were observed under UV excitation (filter set U-MWU2, Olympus, Japan) and counted manually using a reticule grid (10 × 10, 12.5 mm; Spectra Services, Ontario, NY, USA) in a 10× eyepiece (WHN10×, Olympus).

Slides with soil thin sections were placed in a horizontal position and the scale of the microscope stage was used in order to be able to start, and revisit, from the same spot in each parallel soil thin section for better alignment. Cell counts were obtained on counting spots following five lines on each thin section. The first counting line was based on the centre of the glass bead, followed by two lines above and below the first line at a distance of 1 mm, respectively (Figure 1). Four fields of view (henceforth referred as analysed spot) of size

250 μm × 250 μm were counted per spot. The distance between each analysed spot was 1 mm. In total, nine spots per line were analysed on each thin section. The cell counts were extrapolated to cell density; that is, cell counts per area of the counting spot.

To compare the proportion of bacteria determined in thin sections with general cell numbers per gram of bulk sample, an additional set of samples were prepared in a similar way to that described in Section 2.3. The cells were enumerated in dispersed soil samples according to the protocol described by Juyal et al., 2018. Briefly, soil microcosms were suspended in 10 mL of 1× PBS solution; 500 μL of the suspension was fixed in 4% formaldehyde solution in 1× PBS at 4°C for 2.5 hr. The samples were filtered on a polycarbonate filter membrane for performing CARD-FISH. The filter sections were hybridized with HRP-labelled oligonucleotide probes. After hybridization, for tyramide signal amplification the filter sections were incubated with the amplification buffer containing fluorescein-labelled tyramides. After amplification the filter sections were washed in distilled water (dH₂O) and
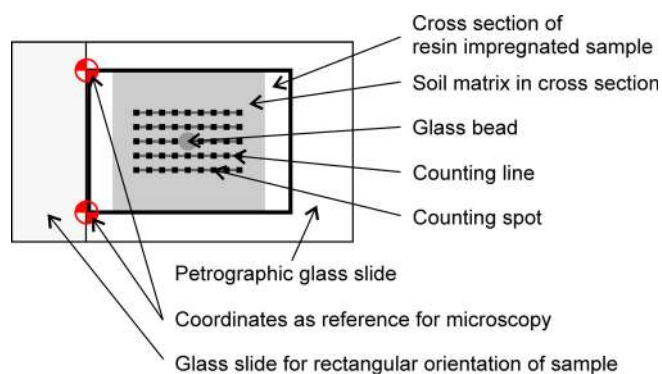
dehydrated with ethanol. The filter sections were mounted with an antifading solution containing DAPI stain on glass slides. The CARD-FISH signals were detected on filter sections under epifluorescence microscopy with a double excitation filter set (#24, Carl Zeiss, Oberkochen, Germany).

2.8 | Image processing and analysis of pore geometry

For image processing a stereomicroscopic image of each soil thin section was taken and used to retrieve the same layer from the image stacks of CT data (Figure 2). The distance of each thin section from the reference side measured was also used. The selected CT image was then cropped to the region of interest of size 1.0 × 1.0 mm (the area where bacterial cells were counted). The cropped region of interest of each thin section was then thresholded using an in-house-developed indicator kriging method (Houston, Otten, Baveye, & Hapca, 2013).

The pore geometry of each soil thin section was analysed at a smaller scale in 3D as described in Juyal et al. (2019). Briefly, the neighbouring slices above and below the selected region of interest (each analysed spot) were considered and cropped down to 1 mm size. In-house-developed software was used to quantify porosity, connectivity and solid-pore interfacial area of the pores, based on voxel data obtained from CT scans (detection limit of 10.87 μm). The porosity was calculated as the volume fraction occupied by pores, whereas connectivity was determined as the volume fraction of pore space that is connected with the external surface of the image volume. The surface area of solid-pore interfaces was estimated using Minkowski functionals, and expressed in relation to the area of solids directly connected to the pore space (Houston et al., 2013).

FIGURE 1 Schematic representation of a soil thin section (vertical cut) used for the enumeration of microbial cells within the soil matrix [Color figure can be viewed at wileyonlinelibrary.com]

FIGURE 2 Example of alignment of a stereomicroscopic image (a) with a computed tomography (CT) image (b). The circle in the middle is the glass bead representing the point of bacteria inoculation. Sample packed at bulk density of 1.3 g cm⁻³. The red frame represents the area used for analysis of both cell counts and pore space analyses. Scale bar: 5 mm [Color figure can be viewed at wileyonlinelibrary.com]
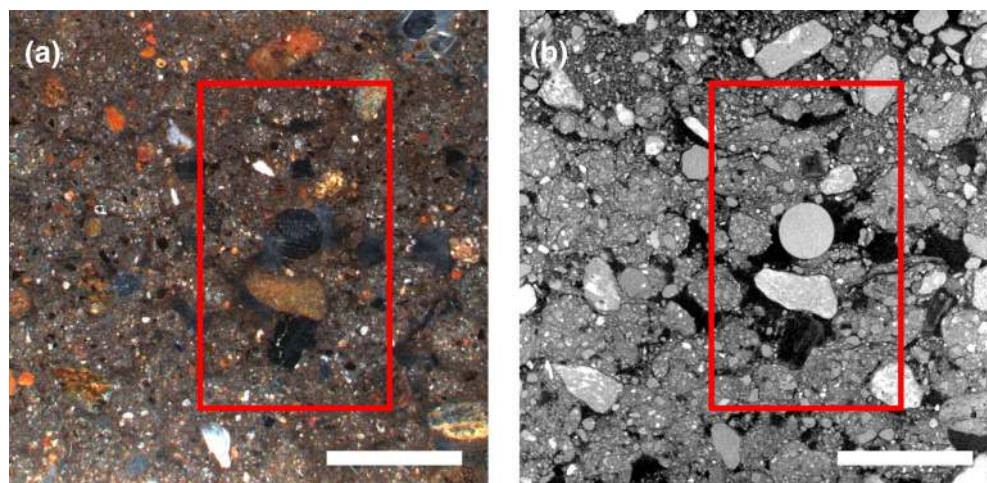
2.9 | Statistical analysis

Statistical analysis was performed using SPSS version 22 (IBM Corp., Armonk, NY, USA). A mixed effect linear model (assuming normal distribution) was used to investigate differences in soil pore characteristics for different treatments, with treatments as fixed factor. The data were assessed for normality first using the Shapiro–Wilk test and secondly by observing normal probability plots and histograms using SPSS. To comply with the normality assumption, the porosity and connectivity measures were transformed using the probit function. The solid-pore interfacial area data met the normality assumption; hence, they did not require any preliminary transformation.

A generalized mixed-effect Poisson model with log link function was used to investigate significant difference in bacterial cell density between different treatments, with soil thin sections and treatments as fixed factors. The effect of soil structure properties such as porosity, connectivity and solid-pore interfacial area on the extent of spread of bacteria was also analysed by a Poisson model with treatments and thin sections as fixed factors. The size of each analysed spot was introduced as an offset variable in the Poisson model.

Statistical analysis of total cell counts in soil thin sections and soil suspensions was performed by a Tukey honestly significant difference (HSD) post-hoc test.

3 | RESULTS

3.1 | Pore characteristics of soil microcosms

The pore characteristics of the two bulk density treatments differed in terms of porosity, connectivity and solid-pore interfacial area (Table S1). The analysis of soil porosity indicated that soil packed at bulk density of 1.3 g cm^{-3} had an average porosity of 24% (standard error (SE) $\pm 1.05\%$) compared to 23% (SE $\pm 0.91\%$) for soil packed at higher bulk density of 1.5 g cm^{-3}; however, the difference was not statistically significant ($p = .612$), which may be a result of the limited resolution in X-ray CT scanning (see 4.1). The difference between the two bulk density treatments in terms of the connectivity of pores was statistically significant ($p = .0456$), with an average connectivity of pores from 94% (SE $\pm 0.55\%$) for soil packed at the lower bulk density to 89% (SE $\pm 0.99\%$) for soil packed at higher bulk density. The solid-pore interfacial area declined with increasing bulk density from 0.05 mm^2 (SE ± 0.001 mm^2) in soil packed at bulk density of 1.3 g cm^{-3} to 0.04 mm^2 (SE ± 0.001 mm^2) in soil packed at bulk density of 1.5 g cm^{-3} ($p = .000$).

3.2 | Enumeration of *Pseudomonas* cells in soil thin sections

Pseudomonas cells stained with DAPI appeared bright blue in colour against a brown-coloured soil background (Figure 3). The *Pseudomonas* cells were mainly observed within the soil matrix or at the solid-pore interfacial area, representing internal aggregate structures and aggregate surfaces, respectively. In the lower bulk density treatment the bacterial cells appeared to be in the form of small group of colonies (Figure 3a), compared to the higher bulk density treatment (Figure 3b). The autofluorescence of some soil compounds did not hamper the enumeration of bacterial cells as they appeared yellowish in colour. Both the treatments showed a substantial variability in the bacterial cell counts at the microscale (Figure 4). *Pseudomonas* cells ranged from 0 to 33 cells per analysed spot in soil with lower bulk density and from 0 to 23 cells
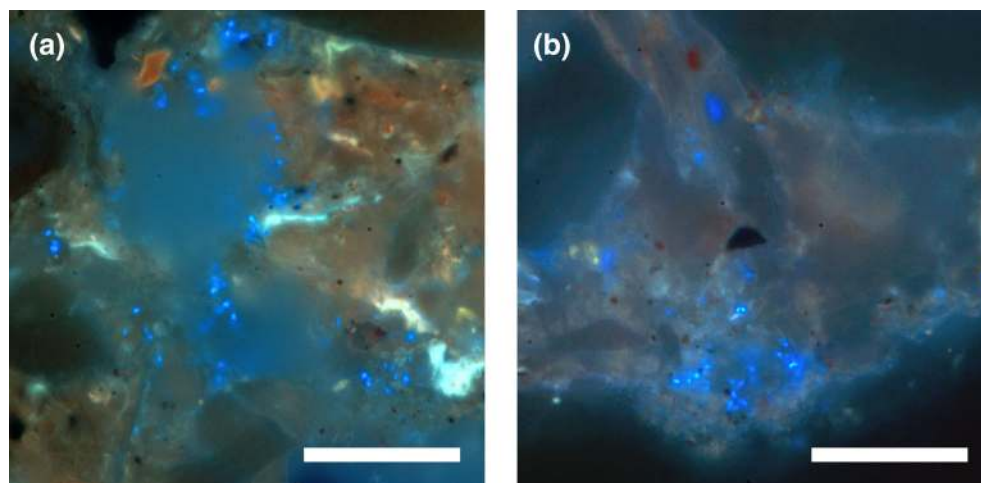

FIGURE 3 Microscopic images of DAPI-stained *Pseudomonas fluorescens* cells in thin sections of soil microcosms packed at (a) 1.3 g cm^{-3} and (b) 1.5 g cm^{-3} bulk density. Bacterial cells are bright blue. Scale bar: 20 μm [Color figure can be viewed at wileyonlinelibrary.com]
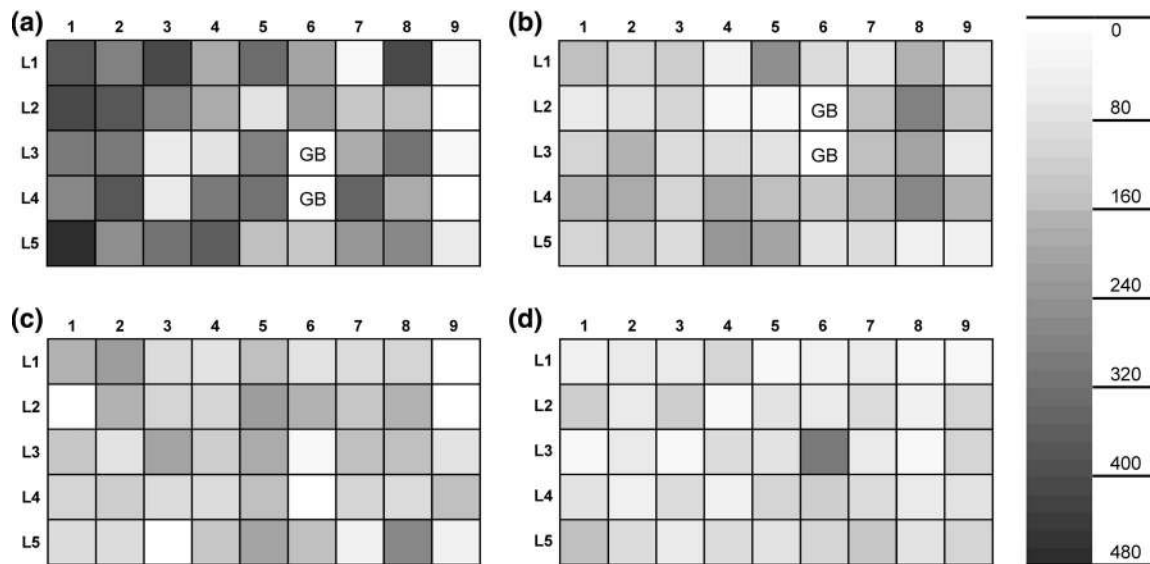
FIGURE 4 Distribution of bacterial cells in vertical thin sections of resin-impregnated soil microcosms with inoculum (*Pseudomonas fluorescens*). Left (a + c): soil microcosm packed at bulk density of 1.3 g cm^{-3}. Right (b + d): soil microcosm packed at bulk density of 1.5 g cm^{-3}. Top (a + b): soil thin section passing through the glass bead. Bottom (2): soil thin section approx. 2.5 mm above the glass bead. 1st column: bottom of the packed soil microcosm. 9th column: top of the packed soil microcosm. Unit of cell densities: cells per mm^2. GB: glass bead. 1 square represents a distance of 1 × 1 mm

per analysed spot in soil with higher bulk density. In control samples, bacterial cells ranged from 0 to 11 in soil with a low bulk density and 0 to 6 in soil with a high bulk density (Figure S5). Most analysed spots were observed to be completely devoid of cells. The proportion of analysed spots without cells was greater in soil packed at bulk density of 1.5 g cm^{-3} compared to soil packed at a bulk density of 1.3 g cm^{-3}.

The average cell density of *Pseudomonas* cells was 42% higher in soil with lower bulk density ($p < .001$) with 174 cells mm^{-2} (SE ±6.3), compared to soil packed at the higher bulk density, which had a bacterial density of 99 cells mm^{-2} (SE ±4.3). In control samples, bacterial cell density was 26 cells mm^{-2} (SE ±4.3) for soil packed at bulk density of 1.3 g cm^{-3} and 14 cells mm^{-2} (SE ±1.1) for soil packed at bulk density of 1.5 g cm^{-3}. Although some bacterial cells were observed in control samples of both the treatments, the difference between the control and inoculated samples was statistically significant ($p < .001$).

The spread rate of *Pseudomonas* at different distances from the inoculum point in soil was affected in both the treatments (Figure 5). The average cell density at a given distance from the inoculum point was higher ($\beta = 3.122$) for the soil packed at lower bulk density (Table 1). Overall, the rate of *Pseudomonas* spread at any given distance from the inoculum point was significantly ($p = .002$) higher in soil packed at lower bulk density compared to soil packed at higher bulk density ($p = .447$). These results confirm that *Pseudomonas* cells dispersed further

TABLE 1 Results of the Poisson model analysis on influence of distance to the bead on the spread of *Pseudomonas fluorescens* cells in soil with different bulk-density treatments

Treatments	*p*-value	Coefficient β
Pseudomonas fluorescens inoculated in soil packed at bulk density 1.3 g cm^{-3}	.002	3.122
Pseudomonas fluorescens inoculated in soil packed at bulk density 1.5 g cm^{-3}	.447	−0.762

Numbers reported in the table are the *p*-values and coefficient values (β) are the estimation of the fixed coefficients of distance in the test model of the analysis.

from the inoculation point source in soils packed at bulk density of 1.3 g cm^{-3} compared to soil packed at bulk density of 1.5 g cm^{-3}.

Cells enumerated on soil thin sections were extrapolated to cells g^{-1} of soil and compared with cell numbers obtained from dispersed samples. In soil packed at lower bulk density respective cell counts were 1.32 × 10^8 (SE ±1.60 × 10^7) cells g^{-1} of soil in dispersed samples and 1.34 × 10^8 (SE ±2.25 × 10^7) cells g^{-1} of soil in thin sections. In soil packed at higher bulk density cell counts were 7.62 × 10^7 (SE ±8.41 × 10^6) cells g^{-1} of soil in dispersed samples and 6.62 × 10^7 (SE ±1.12 × 10^7) cells g^{-1} soil in thin sections (Figures S3 and S4).
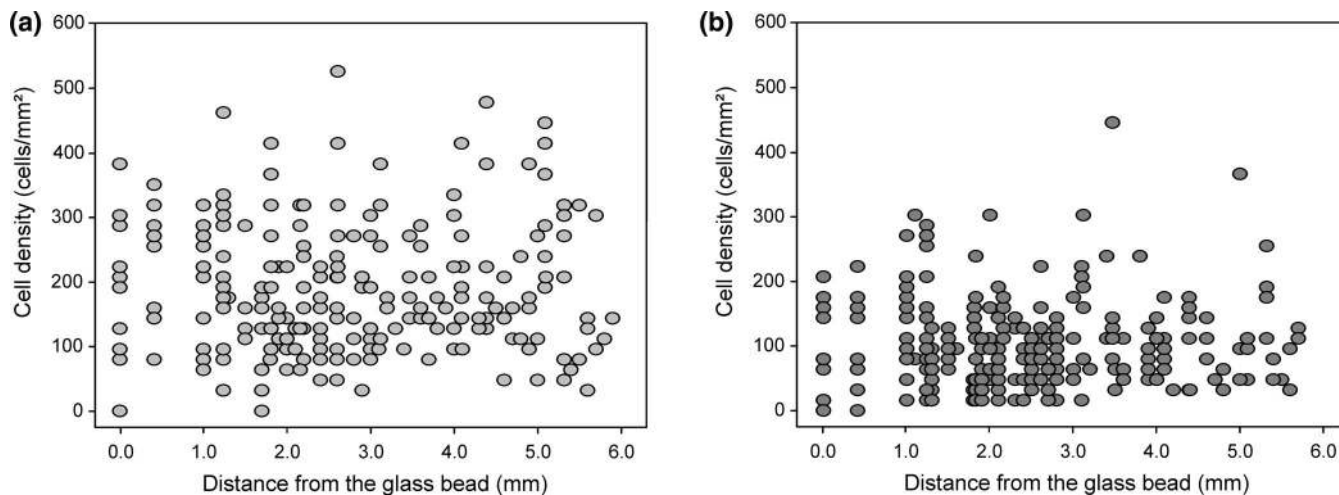
FIGURE 5 Cell densities of *Pseudomonas fluorescens* cells in soil thin sections based on the distance from the glass bead. (a) Packed at bulk density of 1.3 g cm^{-3}. (b) Packed at bulk density of 1.5 g cm^{-3}. Each data point in the graph represents one counting spot analysed in each replicate of a thin section

3.3 | Pore geometry influence on the extent of *Pseudomonas* spread in soil

In Figure 6, the relationships between the soil pore characteristics and bacterial cell density in each analysed spot of the analysed soil thin sections in both bulk density treatments are presented. The influence of soil pore characteristics on the spread of *Pseudomonas* cells differed in soil packed at lower bulk density compared to soil packed at higher bulk density (Table 2). A contrasting influence of soil porosity on the spread of bacteria was observed between the two treatments, with a decrease in cell density ($\beta = -1.453$) in the lower bulk density treatment and an increase in cell density ($\beta = 1.225$) in the higher bulk density treatment. However, the influence was not statistically significant in both the treatments.

Solid-pore interfacial area significantly influenced the spread rate of *Pseudomonas* cells in the lower bulk density treatment. An increase ($\beta = 5.999$) in cell density was observed with greater solid-pore interfacial area (>0.03 mm^2). A slight increase in the cell density ($\beta = 1.034$) with increasing solid-pore interfacial area was also observed in samples of soil packed at higher bulk density; however, the influence was not statistically significant.

The connectivity of pores showed significant influence on the spread of bacteria only in samples packed at lower bulk density, with a slight decrease in cell densities ($\beta = -3.274$) with decreasing connectivity of pores (Figure 6c).

4 | DISCUSSION

In this paper a methodological approach developed in our previous paper (Juyal et al., 2019) was used to investigate the influence of soil pore characteristics on the spatial spread of bacteria from localized nutrients in soil. The introduction of bacteria in the form of an agarose pellet into soil is proposed as a way to introduce bacteria in a solid form compared to the liquid inoculum method used in our previous paper (Juyal et al., 2019). The reason for this is that an addition of liquid suspension of bacterial inoculum would influence spread of introduced bacteria in soil, and water movement would occur and lead to redistribution of bacteria immediately after introduction into the soil. Another advantage of using the solid form is that it provides a reproducible source of inoculum. The introduction of a localized source of inoculum resulted in dispersion of bacteria into the soil largely due to bacterial movement and growth.

4.1 | Enumeration of bacteria in soil thin sections

A difference in cell densities during the 14 days of incubation was observed between the two different bulk density treatments. The detection of bacterial cells in the soil thin sections evidently showed the colonization and spread of bacteria in the surrounding soil area away from the inoculation point. A plausible explanation for this is that *Pseudomonas* spread towards nutrients present in the surrounding areas, as the source of inoculation was nutrient poor compared to the soil. The range of cell counts varied at different distances from the inoculation point. This could be due to the concentration of nutrients available in different regions of soil, for example, nutritional heterogeneity at microscopic scales, but it may also reflect different pathways for spread. Gupta Sood (2003)
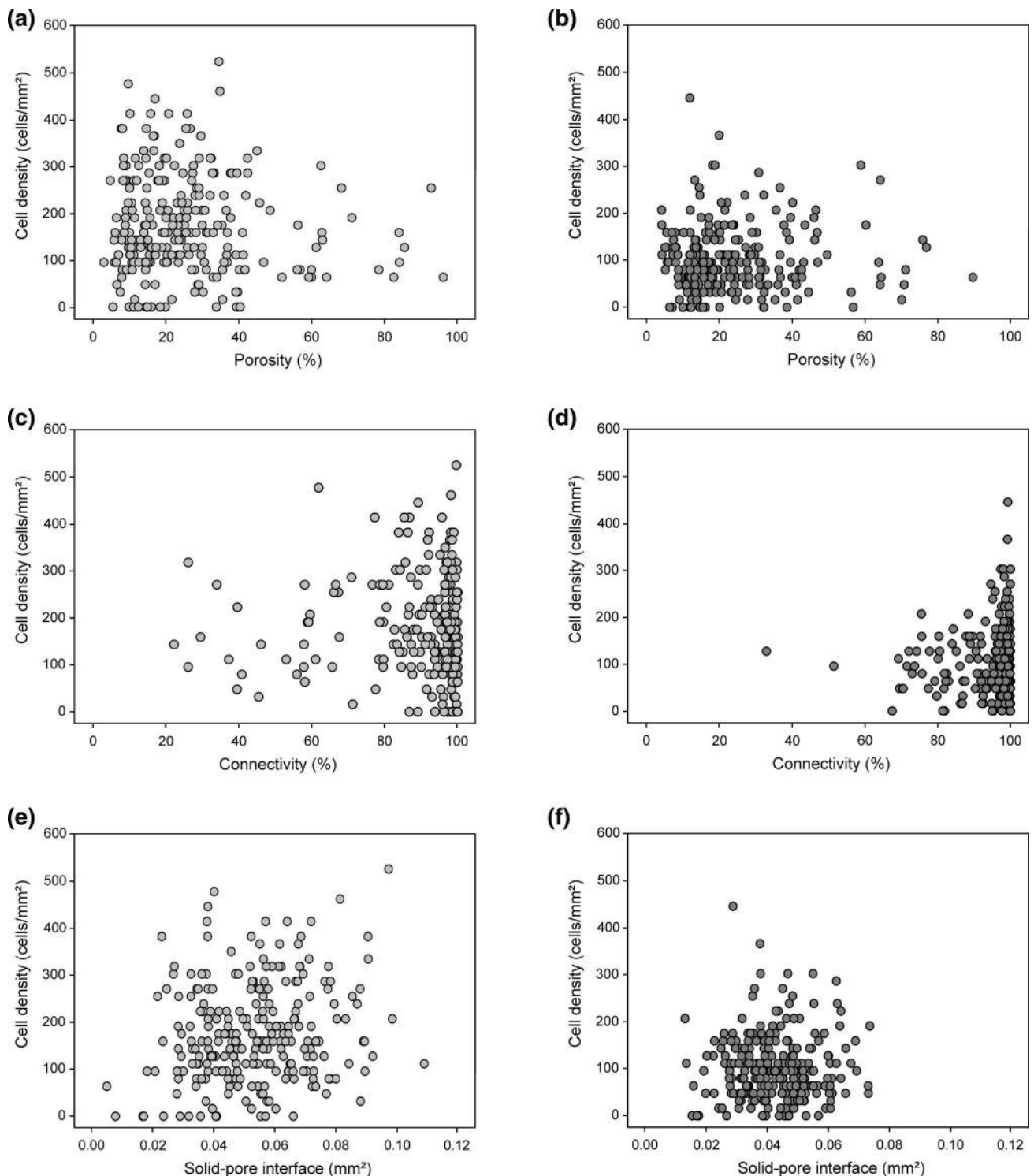
FIGURE 6 Relationship of *Pseudomonas fluorescens* cell density with soil porosity (a + b), connectivity (c + d) and solid-pore interface (e + f) in soil thin sections packed at bulk density of 1.3 g cm^{-3} (left) and 1.5 g cm^{-3} (right). Each data point in the graph represents one counting spot analysed in each replicate of a thin section

showed higher numbers of *Pseudomonas fluorescens* cells attracted towards substances exuded by vesicular-arbuscular mycorrhizal roots compared to non-vesicular-arbuscular mycorrhizal roots. Some other studies (de Weert et al., 2002; Neal, Ahmad, Gordon-Weeks, &

Ton, 2012) have observed a similar higher response of *Pseudomonas* spp. towards substances or metabolites from root exudates of tomato and maize plants.

The average cell density showed high variability in the spread of bacteria at different distances from the

TABLE 2 Results of the Poisson model analysis on influence of pore structure on the spread of *Pseudomonas fluorescens* cells in soil with different bulk-density treatments

	Porosity		Connectivity		Solid-pore interface	
Treatments	*p*-value	Coefficient β	*p*-value	Coefficient β	*p*-value	Coefficient β
Pseudomonas fluorescens inoculated in soil packed at bulk density 1.3 g cm^{-3}	.147	−1.453	0.001	−3.274	.000	5.999
Pseudomonas fluorescens inoculated in soil packed at bulk density 1.5 g cm^{-3}	.222	1.225	0.111	2.571	.302	1.034

Numbers reported in the table are the *p*-values and coefficient values (β) are the estimation of the fixed coefficients (porosity, connectivity and solid-pore interface) in the test model of the analysis.

inoculation point. The cell density was higher in the thin section closer to the inoculation point compared to the other one (2.5 mm away) in both the bulk density treatments. This is likely to be because the distance to access nutrients in soil was shorter in the thin section closer to the inoculation point compared to the other thin section that was further away.

A study by Nunan, Wu, Young, Crawford, and Ritz (2002) showed a high degree of aggregation of bacterial cells in topsoil compared to subsoil. In the present study, the distances between the two sections refers to the different depth of soil. The nutrient distribution between these two thin sections is relevant to the availability of nutrients found in the field soil. Another study by Dechesne, Pallud, Bertolla, and Grundmann (2005) also showed a high variation in the distribution of introduced bacteria *Pseudomonas putida* after addition of substates to soil columns. The length of incubation time can also be another reason for such distribution patterns of bacteria in soil. By the time the microcosms were sampled bacteria would have grown and colonized in the soil closer to the inoculation point (represented by the thin section in the centre of the sample) more than in the other sections.

Growth of introduced *Pseudomonas* cells in soil columns was confirmed by comparing CARD-FISH cell counts in dispersed samples taken 1 and 14 days after inoculation, respectively. The number of DAPI cell counts analysed on soil thin sections was verified by cell enumeration using CARD-FISH (Schmidt, Bengough, Gregory, Grinev, & Otten, 2012) on a set of microcosms, which was incubated in parallel. Cell numbers were in the same range and thus staining and counting using DAPI on polished resin-impregnated samples has proven to be efficient (Figure S3). Bacterial numbers analysed (by CARD-FISH) in dispersed samples of both treatments showed an increase in cell counts on day 14 compared to day 1. For example, *Pseudomonas* cell counts increased from 3.62×10^7 (SE $\pm 3.88 \times 10^6$) on day 1 to 1.32×10^8 (SE $\pm 1.60 \times 10^7$) on day 14 for samples packed at bulk density of 1.3 g cm^{-3} (Figure S4).

Among the two treatments, the hypothesis that increasing bulk density would affect the spread rate of bacteria in soil was confirmed, and a decrease in the spread of bacteria with increasing bulk density was observed. These results are consistent with the findings of our previous work, which showed a decrease in the rate of spread with increasing bulk density over time. The difference in cell density could be due to the alterations in soil pore geometry, which limited the access of bacteria to nutrients in soil as the number of bacteria added in both treatments was the same.

The pore characteristics of each analysed spot where bacteria were counted were also analysed. Results showed that only connectivity and the solid-pore interfacial area of pores were affected by increasing bulk density. Soil porosity determined by X-ray CT was quite similar for both bulk density treatments. This may be because the pores analysed here were limited to the scanning resolution; that is, only pores greater than 10.87 μm were analysed. For example, the total porosity of a sample packed at bulk density of 1.3 g cm^{-3} is 48% and of soil packed at bulk density of 1.5 g cm^{-3} is 40% (calculated based on bulk density and particle density). However, the porosity determined by X-ray CT scanned at a resolution of 10.87 μm resulted in 24% for soil packed at a bulk density of 1.3 g cm^{-3} and 23% for soil packed at bulk density of 1.5 g cm^{-3}. This means that around 42–50% of the total porosity is not detected by the scanner. Therefore, the conclusions made in this study on the pore characteristics are based on the pores greater than the detection limit.

However, the pores analysed are more relevant to the present study as the larger pores will affect the distribution of water and the air-water interface, the diffusion pathways of dissolved organic carbon and the diffusion pathways of oxygen and hence can be expected to affect the growth and spread of bacteria in different treatments. Moreover, fine micropores (≤ 0.2 μm in diameter) are less relevant for this study as they represent non-habitable pore space (Hassink, Bouwman, Zwart, & Brussard, 1993). As these pores are estimated to account for 14% and 12% at 1.3 g cm^{-3} and 1.5 g cm^{-3} bulk density, respectively (Ad-hoc-AG Boden, 2005), only 5–10% of the pores that were relevant for this study could not be detected via CT. This is

consistent with the study by Juyal et al. (2018), who showed that the larger pores determined by X-ray CT had a significant impact on the growth and spread of bacteria.

4.2 | Influence of pore characteristics on *Pseudomonas* spread

To investigate if the pore geometry did influence the spread rate of bacteria in soil, pore characteristics of each analysed spot were analysed at the microscale. Soil porosity did not show a significant influence on the extent of *Pseudomonas* spread in soil. This could be because of the scale of observation with X-ray CT, which visualized pores that were air-filled prior to resin impregnation, whereas the majority of bacteria were located in pores that were water filled. The connectivity of pores showed a significant influence on the spread of bacteria only in loosely packed soil. A decrease in connectivity of pores with increase in bulk density could have resulted in limited access to nutrients, water movement and gas exchange.

In a few analysed spots bacterial cells were observed in 0% of connected pores. As connectivity is required for bacteria to move, it is most likely that these pores are connected through pores below the scanning resolution, but large enough for bacteria to move through. Therefore, to avoid biased results we excluded the cell count data observed at 0% connected pores. A significant influence of the solid-pore interfacial area of pores on bacterial cell spread rate was observed in the lower bulk density treatment. A plausible explanation for this is that at lower bulk density nutrients might have been readily accessible to bacteria as they are transported through soil and, therefore, bacteria might have colonized near the vicinity of these pores. It may also be that in partially saturated soil, water is retained on the surfaces as thin films to accommodate introduced bacterial cells (Carminati, Kaestner, Lehmann, & Flühler, 2008). In addition, bacteria tend to grow on the surfaces of substrates, as can be seen from the soil thin sections (Figure 3). The consequence of this result is that if pore geometry affects the spread and colonization of bacteria at the microscale, it will also affect the activity of microbes in soil. This shows that the pore characteristics control the access of nutrients in soil. Strong, De Wever, Merckx, and Recous (2004) showed that the rate of decomposition of organic C depends on the location in the soil pore network. Ruamps, Nunan, and Chenu (2011) also showed that decomposition of organic carbon and microbial community structure varies in pores of different size classes in soil. In the present study some of the soil pore characteristics, such as porosity and solid-pore interfacial area,

showed a significant influence on the extent of bacterial spread in soil at the microscale.

Thus, the method developed in the present study can be used to study how introduced bacteria contact their target through soil to carry out activities such as promoting plant growth or mineralization of soil pollutant. The study highlights how the physical factors (bulk density in this case) expected to influence the distribution of microorganisms at macroscopic scales vary at the microscopic scale. Therefore, this study shows the importance of studying the parameters affecting the activity of microorganisms in soil at scales relevant to microbes.

5 | CONCLUSION

In this study, we provide evidence that bacteria spread though soil in the absence of water movement. We also showed that soil physical conditions and pore architecture in particular affect the rate and extent of spread of bacteria through soil. The rate of spread of *Pseudomonas* bacteria was faster in soil packed at lower bulk density compared to soil packed at higher bulk density. Analysis of X-ray CT images of soil thin sections of samples packed at lower and higher bulk density revealed that the rate of spread of bacteria was influenced by connectivity of soil pores and the solid-pore interfacial area at the lower bulk density. This study thus suggests that soil structure can affect the growth and spread of bacteria and thus their activity. Information collected from this methodological approach can be used to build mathematical models to explore the link between microbial community activities and various soil parameters, such as explored by Portell, Pot, Garnier, Otten, and Baveye (2018). Further research is therefore required to study the complete effects of physical, chemical and biological properties on the microbial processes in soil for better soil management.

CONFLICT OF INTEREST
None.

DATA AVAILABILITY STATEMENT

The underlying data can be accessed through the Cranfield University data repository at http://doi.org/10.17862/cranfield.rd.11854239

ORCID

Archana Juyal https://orcid.org/0000-0003-1993-245X
Wilfred Otten https://orcid.org/0000-0002-3847-9825
Philippe C. Baveye https://orcid.org/0000-0002-8432-6141
Thilo Eickhorst https://orcid.org/0000-0003-0436-9895

REFERENCES

Baveye, P. C., Otten, W., Kravchenko, A., Balseiro-Romero, M., Beckers, É., Chalhoub, M., ... Kiryanyaz, S. (2018). Emergent properties of microbial activity in heterogeneous soil microenvironments: Different research approaches are slowly converging, yet major challenges remain. *Frontiers in Microbiology*, *9*, 1929.

Boden, A.-h.-A G. (Ed.). (2005). *Bodenkundliche Kartieranleitung* (5th ed.). Stuttgart: E. Schweizerbart'sche Verlagsbuchhandlung.

Burd, G. I., Dixon, D. G., & Glick, B. R. (2000). Plant growth-promoting bacteria that decrease heavy metal toxicity in plants. *Canadian Journal of Microbiology*, *46*(3), 237–245.

Carminati, A., Kaestner, A., Lehmann, P., & Flühler, H. (2008). Unsaturated water flow across soil aggregate contacts. *Advances in Water Resources*, *31*(9), 1221–1232.

de Weert, S., Vermeiren, H., Mulders, I. H. M., Kuiper, I., Hendrickx, N., Bloemberg, G. V., ... Lugtenberg, B. J. J. (2002). Flagella-driven Chemotaxis towards exudate components is an important trait for tomato root colonization by *Pseudomonas fluorescens*. *Molecular Plant-Microbe Interactions*, *15*(11), 1173–1180.

Dechesne, A., Pallud, C., Bertolla, F., & Grundmann, G. L. (2005). Impact of the microscale distribution of a Pseudomonas strain introduced into soil on potential contacts with indigenous bacteria. *Appl Environ Microbiol*, *71*, 8123–8131.

Ekschmitt, K., Liu, M., Vetter, S., Fox, O., & Wolters, V. (2005). Strategies used by soil biota to overcome soil organic matter stability — Why is dead organic matter left over in the soil? *Geoderma*, *128*, 167–176.

Gupta Sood, S. (2003). Chemotactic response of plant-growth-promoting bacteria towards roots of vesicular-arbuscular mycorrhizal tomato plants. *FEMS Microbiology Ecology*, *45*, 219–227.

Hapca, S., Baveye, P. C., Wilson, C., Lark, R. M., & Otten, W. (2015). Three-dimensional mapping of soil chemical characteristics at micrometric scale by combining 2D SEM-EDX data and 3D X-ray CT images. *PLoS One*, *10*(9), e0137205.

Hassink, J., Bouwman, L. A., Zwart, K. B., & Brussard, L. (1993). Relationships between habitable pore space, soil biota and mineralization rates in grassland soils. *Soil Biology and Biochemistry*, *25*, 47–55.

Hayat, R., Ali, S., Amara, U., Khalid, R., & Ahmed, I. (2010). Soil beneficial bacteria and their role in plant growth promotion: A review. *Annals of Microbiology*, *60*, 579–598.

Houston, A. N., Otten, W., Baveye, P. C., & Hapca, S. (2013). Adaptive-window indicator kriging: A thresholding method for computed tomography images of porous media. *Computers & Geosciences*, *54*, 239–248.

Houston, A. N., Schmidt, S., Tarquis, A. M., Otten, W., Baveye, P. C., & Hapca, S. (2013). Effect of scanning and image reconstruction settings in X-ray computed microtomography on quality and segmentation of 3D soil images. *Geoderma*, *207*, 154–165.

Juyal, A., Eickhorst, T., Falconer, R., Baveye, P. C., Spiers, A., & Otten, W. (2018). Control of pore geometry in soil microcosms and its effect on the growth and spread of *Pseudomonas* and *Bacillus* sp. *Frontiers in Environmental Sciences*, *6*, 1–12.

Juyal, A., Otten, W., Falconer, R., Hapca, S., Schmidt, H., Baveye, P. C., & Eickhorst, T. (2019). Combination of techniques to quantify the distribution of bacteria in their soil microhabitats at different spatial scales. *Geoderma*, *334*, 165–174.

King, E. O. Ward, M. K., & Raney, D. E. (1954). Two simple media for the demonstration of pyocyanin and fluorescin. *The Journal of Laboratory and Clinical Medicine*, *44*, 301–307.

Kizungu, R., Grundmann, G. L., Dechesne, A., Bartoli, F., Flandrois, J. P., & Chasse, J. L. (2001). Spatial modeling of nitrifier microhabitats in soil. *Distribution*, *1709*, 1709–1716.

Kuzyakov, Y., & Blagodatskaya, E. (2015). Microbial hotspots and hot moments in soil: Concept & review. *Soil Biology and Biochemistry*, *83*, 184–199.

Madigan, M. T., Clark, D. P., Stahl, D., & Martinko, J. M. (2010). *Brock biology of microorganisms* (13th ed.). San Francisco, CA: Benjamin Cummings.

Neal, A. L., Ahmad, S., Gordon-Weeks, R., & Ton, J. (2012). Benzoxazinoids in root exudates of maize attract pseudomonas putida to the rhizosphere. *PLoS One*, *7*(4), e35498.

Nunan, N., Wu, K., Young, I. M., Crawford, J. W., & Ritz, K. (2002). In situ spatial patterns of soil bacterial populations, mapped at multiple scales, in an arable soil. *Microbial Ecology*, *44*, 296–305.

Nunan, N., Wu, K., Young, I. M., Crawford, J. W., & Ritz, K. (2003). Spatial distribution of bacterial communities and their relationships with the micro-architecture of soil. *FEMS Microbiology Ecology*, *44*, 203–215.

Portell, X., Pot, V., Garnier, P., Otten, W., & Baveye, P. C. (2018). Microscale heterogeneity of the spatial distribution of organic matter can promote bacterial biodiversity in soils: Insights from computer simulations. *Frontiers in Microbiology*, *9*, 1583.

Ruamps, L. S., Nunan, N., & Chenu, C. (2011). Microbial biogeography at the soil pore scale. *Soil Biology and Biochemistry*, *43*, 280–286.

Schlüter, S., Henjes, S., Zawallich, J., Bergaust, L., Horn, M., Ippisch, O., & Dörsch, P. (2018). Denitrification in soil aggregate analogues - effect of aggregate size and oxygen diffusion. *Frontiers in Environmental Science*, *6*, 17.

Schmidt, S., Bengough, A. G., Gregory, P. J., Grinev, D. V., & Otten, W. (2012). Estimating root-soil contact from 3D X-ray microtomographs. *European Journal of Soil Science*, *63*, 776–786.

Strong, D. T., De Wever, H., Merckx, R., & Recous, S. (2004). Spatial location of carbon decomposition in the soil pore system. *European Journal of Soil Science.*, *55*, 739–750.

Vieublé Gonod, L., Chadoeuf, J., & Chenu, C. (2006). Spatial distribution of microbial 2, 4-dichlorophenoxy acetic acid mineralization from field to microhabitat scales. *Soil Science Society of America Journal*, *70*, 64–71.

Young, I. M., Crawford, J. W., Nunan, N., Otten, W., & Spiers, A. (2008). Microbial distribution in soils: Physics and scaling. *Advances in Agronomy*, *100*, 81–121.

Zaidi, A., Khan, M. S., Ahemad, M., & Oves, M. (2009). Plant growth promotion by phosphate solubilizing bacteria. *Acta Microbiologica et Immunologica Hungarica*, *56*, 263–284.

Zhuang, X., Chen, J., Shim, H., & Bai, Z. (2007). New advances in plant growth-promoting rhizobacteria for bioremediation. *Environment International*, *33*, 406–413.

SUPPORTING INFORMATION

Additional supporting information may be found online in the Supporting Information section at the end of this article.